

Absorption of Axion Dark Matter in a Magnetized Medium

Asher Berlin^{✉*} and Tanner Trickle^{✉†}

Theoretical Physics Division, Fermi National Accelerator Laboratory, Batavia, Illinois 60510, USA

 (Received 5 June 2023; revised 5 January 2024; accepted 20 March 2024; published 30 April 2024)

Detection of axion dark matter heavier than an meV is hindered by its small wavelength, which limits the useful volume of traditional experiments. This problem can be avoided by directly detecting in-medium excitations, whose $\sim\text{meV}$ – eV energies are decoupled from the detector size. We show that for any target inside a magnetic field, the absorption rate of electromagnetically coupled axions into in-medium excitations is determined by the dielectric function. As a result, the plethora of candidate targets previously identified for sub-GeV dark matter searches can be repurposed as broadband axion detectors. We find that a kg yr exposure with noise levels comparable to recent measurements is sufficient to probe parameter space currently unexplored by laboratory tests. Noise reduction by only a few orders of magnitude can enable sensitivity to the QCD axion in the ~ 10 meV– 10 eV mass range.

DOI: [10.1103/PhysRevLett.132.181801](https://doi.org/10.1103/PhysRevLett.132.181801)

Introduction.—Despite constituting roughly 27% of the energy density of the Universe [1], the fundamental nature of dark matter (DM) remains elusive. Of the theoretically motivated DM candidates, the QCD axion is particularly remarkable since its existence would also solve the long-standing strong CP problem [2–5]. A generic feature of QCD axion DM models is a coupling between the axion field a and electromagnetism,

$$\mathcal{L} \supset -\frac{1}{4} g_{a\gamma\gamma} a F^{\mu\nu} \tilde{F}_{\mu\nu} = g_{a\gamma\gamma} a \mathbf{E} \cdot \mathbf{B}. \quad (1)$$

In the presence of a static magnetic field \mathbf{B}_0 , the interaction in Eq. (1) converts an axion to an oscillating electromagnetic field [6]. Directly detecting this field is the underlying principle of many ongoing and planned experiments [7]. Traditional detection schemes utilize cavities with electromagnetic modes resonantly matched to axion masses of $m_a \sim (10^{-6} - 10^{-5})$ eV, as motivated by postinflationary misalignment production and a standard cosmological history [8–12]. However, searches across a larger parameter space are motivated by alternative production mechanisms [13–33] and axions that couple to the standard model (SM) similar to the QCD axion but without the strict connection between coupling strength and mass [34–44].

Cavities are an exceptional tool to search for axion DM. However, they are fundamentally limited in the axion mass that they can probe. This is because the axion mass must be

matched to a resonant frequency of the cavity, which is inversely related to its size. Therefore, to resonantly search for higher axion masses, the cavity must be prohibitively small, limiting the total exposure. Recent strategies to boost exposure to high-mass axions include nonresonant detection of single photons in a large volume dish antenna [45], and modifications to the photon’s dispersion relation in dielectric [46–48] or plasma [49–51] structures tuned to a specific mass.

While these searches are focused on photon detection, another possibility is to directly detect the in-medium excitations in crystal targets involving, e.g., electrons [52–80], phonons [76,77,81–87], and magnons [82,88–92]. Since the energy of these modes ($\sim\text{meV}$ – eV) is not set by the target size, but rather by the physics of the local environment, they are ideal for high-mass axion searches. Furthermore, the manufacturing of low-noise targets and the technology required to detect single quanta of such excitations is at the forefront of the DM direct detection community and is thus an active area of development [93]. In particular, current experiments, such as CDEX [94], DAMIC [95–99], EDELWEISS [100–102], SENSEI [103–105], and SuperCDMS [106–108], utilize eV-scale electronic excitations in Si and Ge targets. More novel targets with sub-eV electronic excitations have also been proposed, such as narrow gap semiconductors [109], Dirac materials [61,63,65,69–72], spin-orbit coupled materials [57,79], and doped semiconductors [73]. Additionally, phonon excitations have been studied in a wide variety of target materials [76,80,82–85,110], including GaAs and Al_2O_3 as planned for the TESSARACT experiment [111].

In this Letter, we demonstrate that the entirety of these ideas can be used to search for the axion-photon coupling in Eq. (1), provided that the target can be placed inside a magnetic field, thus creating a “magnetized medium.”

Published by the American Physical Society under the terms of the Creative Commons Attribution 4.0 International license. Further distribution of this work must maintain attribution to the author(s) and the published article’s title, journal citation, and DOI. Funded by SCOAP³.

In particular, we show that in a magnetized medium the inclusive axion absorption rate into in-medium excitations is directly related to the dielectric function. While previous work has shown that the dielectric function dictates the absorption rate into photons mixing with plasmon [49–51] and phonon [87] excitations, here we show that this relationship is universal and provides a compact expression for the inclusive absorption rate directly into any such in-medium excitation. This is important both experimentally, since the dielectric can be measured, and theoretically, because it broadly captures the absorption rate into any in-medium excitation, abstracting away from calculations specific to any single excitation. This allows us to easily evaluate the sensitivity of various materials, as well as identify a larger scope of relevant signals that have previously been overlooked, such as low-energy electronic excitations. Below, we begin by deriving the absorption rate with two methods. The first derivation involves self-energies, analogous to calculations performed in the context of direct detection experiments; the second is provided within the language of classical axion electrodynamics. These derivations provide complementary ways to understand the underlying physics. We then discuss the projections shown in Fig. 1, which illustrate the promising ability to explore new, high-mass, QCD axion parameter space.

Absorption rate.—Before deriving the rate for axion absorption in a magnetized medium, we begin with a synopsis of the final result for isotropic targets. The total axion absorption rate, per unit exposure, is given by

$$R \simeq \left(\frac{g_{a\gamma\gamma} B_0}{m_a} \right)^2 \frac{\rho_{\text{DM}}}{\rho_{\text{T}}} \text{Im} \left[\frac{-1}{\epsilon(m_a)} \right], \quad (2)$$

where $\rho_{\text{DM}} \simeq 0.4 \text{ GeV}/\text{cm}^3$ is the local axion DM energy density, ρ_{T} is the mass density of the target, and $\epsilon(m_a)$ is the dielectric function evaluated at energy $\omega = m_a$ and momentum deposition $q = 0$, appropriate for absorption kinematics ($q \ll \omega$) which are assumed throughout [119]. The former process is governed by the strength of the external magnetic field and $g_{a\gamma\gamma}$, while the latter is determined by the dielectric function, independent of both the axion physics and, in the $q \ll \omega$ limit, the magnetic permeability. This separability is advantageous since, in principle, the dielectric function of the target can be measured directly. In the absence of measurement, this parametrization is useful as a bridge between particle physics and first-principles condensed matter calculations. First-principles calculations are a useful tool to understand the contributions of individual excitations, which cannot be understood from a measurement of the inclusive dielectric function. However, this generally ceases to be a problem when the various excitations are sufficiently separated in energy, e.g., in typical semiconductors where phonon excitations are $\mathcal{O}(\text{meV})$ and electronic excitations are $\mathcal{O}(\text{eV})$.

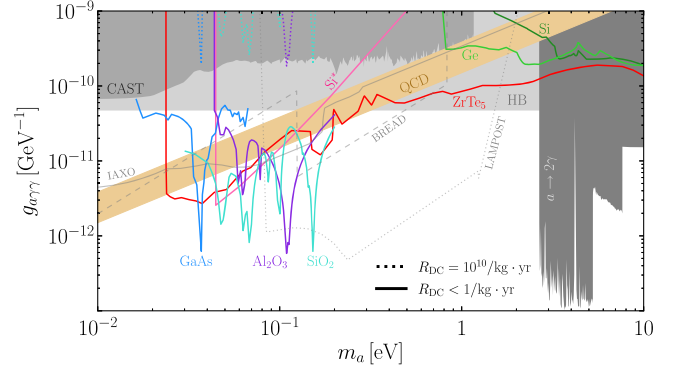


FIG. 1. Projected sensitivity to electromagnetically coupled axion DM for a kg yr exposure of various targets inside a 10 T magnetic field. Solid colored lines assume negligible backgrounds, and dotted colored lines assume a dark count (DC) rate of $R_{\text{DC}} = 10^{10}/\text{kg} \cdot \text{yr}$. Targets utilizing single-phonon excitations include GaAs (light blue) and Al_2O_3 (purple) (proposed for the TESSARACT experiment [111]), as well as SiO_2 (turquoise). The Si (dark green) and Ge (light green) targets correspond to single-electron excitations currently searched for by the CDEX [94], DAMIC [95–99], EDELWEISS [100–102], SENSEI [103–105], and SuperCDMS [106–108] experiments. Doped Si (Si^* , pink) [73] and ZrTe_5 (red) [57] correspond to novel targets utilizing low-energy electronic excitations. Shaded gray regions are existing limits derived from horizontal branch (HB) star cooling [112], the CAST helioscope [113,114], and searches for $a \rightarrow 2\gamma$ decays by the MUSE [115], HST [116], and VIMOS [117] telescopes. Also shown as gray lines are projections from the IAXO (solid) [118], BREAD (dashed) (assuming DCs of $\sim 10^4$ or $\lesssim 1$ for masses below or above $\sim 100 \text{ meV}$, respectively, over 10^3 days) [45], and LAMPOST (dotted) (assuming approximately ten DCs per 10^6 s run and $\sim 10^4$ runs) [48] experiments. The orange band denotes the range of couplings and masses as motivated by the QCD axion.

The idea of relating the dielectric function to the DM absorption rate into in-medium excitations has been used for other DM models [52–54,56,79,80], as well as in calculations of the DM absorption rate into in-medium photon states [50,51,122]. For example, for kinetically mixed dark photon DM A' , the absorption rate into in-medium excitations is [52,56,80]

$$R \simeq \kappa^2 \frac{\rho_{\text{DM}}}{\rho_{\text{T}}} \text{Im} \left[\frac{-1}{\epsilon(m_{A'})} \right], \quad (3)$$

where κ is the kinetic-mixing parameter and $m_{A'}$ is the A' mass. The similarity between the dark photon absorption rate in Eq. (3) and the axion absorption rate in Eq. (2) is immediately clear. As a result, for DM particles of the same mass, the sensitivity to electromagnetically coupled axions can be simply rescaled via the mapping $g_{a\gamma\gamma} B_0 \leftrightarrow \kappa m_a$ corresponding to

$$g_{a\gamma\gamma} \sim 10^{-10} \text{ GeV}^{-1} \times \left(\frac{\kappa}{10^{-14}} \right) \left(\frac{m_a}{\text{meV}} \right) \left(\frac{T}{B_0} \right). \quad (4)$$

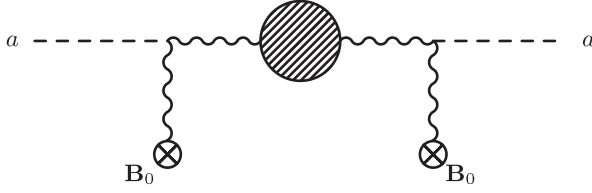


FIG. 2. An illustrative Feynman diagram for the axion a self-energy in a magnetized medium. The optical theorem relates the imaginary part of this diagram to the axion absorption rate. The external magnetic field \mathbf{B}_0 is represented as a background source, and the shaded “blob” represents any in-medium modification to the photon propagator (e.g., from electron and phonon excitations).

We now turn to the details of the calculation, beginning with a self-energy treatment similar to Refs. [53,56,123], then turning to an alternative derivation employing classical equations of motion similar to Refs. [87,124].

Self-energy calculation.—The starting point of the self-energy derivation is the optical theorem, which relates the absorption rate of a particle to the imaginary part of its self-energy. The self-energy can then be computed diagrammatically. The relevant Feynman diagram for axion absorption in a magnetized medium is shown in Fig. 2; the vertex Feynman rule is derived from the Lagrangian in Eq. (1), and the photon propagator is modified due to the presence of the medium. Following Refs. [56,123], the probability of axion absorption per unit time is given by

$$\Gamma \simeq -\frac{1}{m_a} \sum_{\lambda} \text{Im} \left[\frac{\Pi_{aA}^{\lambda} \Pi_{AA}^{\lambda}}{m_a^2 - \Pi_{AA}^{\lambda}} \right], \quad (5)$$

where the diagram in Fig. 2 has been decomposed into the 1PI diagrams Π_{aA} , Π_{Aa} , and Π_{AA} , i.e., the diagrams with no internal, cuttable, a or A lines. Π_{AA}^{λ} is the self-energy of A projected onto the λ th polarization e_{μ}^{λ} defined to diagonalize $\Pi_{AA}^{\mu\nu}$: $\Pi_{AA}^{\lambda} = -e_{\mu}^{\lambda} \Pi_{AA}^{\mu\nu} e_{\nu}^{\lambda}$. Π_{aA}^{λ} is the self-energy mixing a and A projected onto the same photon polarization vector, i.e., $\Pi_{aA}^{\lambda} = -e_{\mu}^{\lambda} \Pi_{aA}^{\mu}$. Note that Eq. (5) is only valid in the absence of direct axion-electron couplings. This is a valid approximation when axioelectric absorption [52,56,125] is subdominant, i.e., when $g_{aee} \ll g_{a\gamma\gamma} e B_0 / m_a^2$ [126], where g_{aee} is the dimensionful axion-electron coupling of the form $\mathcal{L} \supset g_{aee} \partial_{\mu} a \bar{e} \gamma^{\mu} e$. For the benchmark DFSZ and KSVZ QCD axion models, in which the axion acquires tree-level or radiatively generated couplings to SM fermions, respectively (see, e.g., Ref. [127] for a review), this is equivalent to

$$m_a \lesssim \left(\frac{B_0}{10 \text{ T}} \right)^{1/2} \times \begin{cases} 2 \text{ eV} / \sin \beta & (\text{DFSZ}), \\ 200 \text{ eV} & (\text{KSVZ}), \end{cases} \quad (6)$$

where $\tan \beta$ is the ratio of the up- and down-type Higgs doublet vacuum expectation values in the DFSZ model. This

is easily satisfied within the parameter space of interest in this work.

We now compute the self-energies in Eq. (5). Since the Ward identities [$Q_{\mu} \Pi_{AA}^{\mu\nu} = Q_{\mu} \Pi_{aA}^{\mu} = 0$, where $Q^{\mu} = (\omega, \mathbf{q})$] relate the temporal and spatial components, only Π_{AA}^{ij} and Π_{aA}^i need to be computed. The photon self-energy is determined by the dielectric tensor ϵ^{ij} through $\Pi_{AA}^{ij} = -\omega^2 (1 - \epsilon^{ij})$. Note that the spatial component of the photon polarization vectors diagonalize the dielectric tensor $\epsilon^{ij} = \sum_{\lambda} \epsilon_{\lambda} e_{\lambda}^i e_{\lambda}^j$, where $\epsilon_{\lambda} \equiv e_{\lambda}^i \epsilon^{ij} e_{\lambda}^j$, such that $\Pi_{AA}^{\lambda} \simeq \omega^2 (1 - \epsilon_{\lambda})$. The axion-photon self-energies are determined by the term in Eq. (1) involving the vector potential $g_{a\gamma\gamma} \dot{\mathbf{A}} \cdot \mathbf{B}_0$, and therefore $\Pi_{aA}^i = i g_{a\gamma\gamma} m_a B_0^i = -\Pi_{AA}^i$. Substituting Π_{AA} and Π_{aA} into Eq. (5), and taking the $q \rightarrow 0$ limit, results in

$$\Gamma \simeq \frac{g_{a\gamma\gamma}^2}{m_a} \sum_{\lambda} (\mathbf{e}_{\lambda} \cdot \mathbf{B}_0)^2 \text{Im} \left[\frac{-1}{\epsilon_{\lambda}(m_a)} \right]. \quad (7)$$

This expression can be further simplified in the limit of an isotropic target. The dielectric of an isotropic target is independent of polarization $\epsilon_{\lambda} = \epsilon$, and the photon polarization vectors are the standard transverse $e_{\pm}^{\mu} = (0, \hat{\mathbf{q}}_{\pm})$ and longitudinal $e_L^{\mu} = (q, \omega \hat{\mathbf{q}}) / \sqrt{Q^2}$ ones, where $\hat{\mathbf{q}}_{\pm}$ are two vectors mutually orthonormal to $\hat{\mathbf{q}}$. The sum over polarizations can be performed using $\sum_{\lambda} e_{\lambda}^i e_{\lambda}^j = \delta^{ij}$. Applying these approximations, Eq. (7) simplifies to

$$\Gamma \simeq \frac{(g_{a\gamma\gamma} B_0)^2}{m_a} \text{Im} \left[\frac{-1}{\epsilon(m_a)} \right]. \quad (8)$$

Similar simplifications occur if the direction of \mathbf{B}_0 is averaged over. The rate per unit exposure R in Eq. (2) is then obtained by multiplying Γ by the number of axions in the target and dividing by the target mass.

Classical equations of motion.—Alternatively, the absorption rate can be derived using classical axion electrodynamics. Throughout, we will implicitly work in the Lorenz gauge. Our starting point is the wave equation for the vector potential, which is approximately $\epsilon; \partial_t^2 \mathbf{A} \simeq \mathbf{j}_a$, where $\mathbf{j}_a = g_{a\gamma\gamma} \dot{\mathbf{A}} \mathbf{B}_0$ is the axion effective current and $\epsilon;$ is the dielectric tensor. This equation is trivially solved for \mathbf{A} by switching to momentum space and projecting onto the photon polarization vectors \mathbf{e}_{λ} , which determines the corresponding electric field to be

$$\mathbf{E} \simeq -g_{a\gamma\gamma} a \sum_{\lambda} \frac{(\mathbf{e}_{\lambda} \cdot \mathbf{B}_0)}{\epsilon_{\lambda}} \mathbf{e}_{\lambda}. \quad (9)$$

The rate for axion absorption is governed by the axion equation of motion, which is approximately

$$(\partial_t^2 + m_a^2) a \simeq g_{a\gamma\gamma} \mathbf{E} \cdot \mathbf{B}_0, \quad (10)$$

with \mathbf{E} given by Eq. (9). The probability per unit time for axion absorption is determined by solving for the imaginary component of the axion frequency in Eq. (10), $\Gamma \simeq \text{Im}(-\omega^2)/m_a$. This leads to a result in agreement with Eq. (7).

Projected sensitivity.—The sensitivity of a variety of targets under the isotropic approximation is shown in Fig. 1, assuming a kg yr exposure and an optimistic $B_0 = 10$ T. In our estimates, we demand $N > 3\sqrt{1 + N_{\text{DC}} + \delta^2 N_{\text{DC}}^2}$, where $N = RM_{\text{T}}t$ and $N_{\text{DC}} = R_{\text{DC}}M_{\text{T}}t$ are the number of signal events and dark counts (DCs), respectively, R_{DC} is the DC rate, M_{T} is the target mass, t is the exposure time, and $\delta \leq 1$ is the systematic uncertainty in the DC. In the absence of background $N_{\text{DC}} \ll 1$, the sensitivity to the axion-photon coupling scales as $g_{a\gamma} \propto (M_{\text{T}}t)^{-1/2}B_0^{-1}$. If backgrounds are instead significant, $N_{\text{DC}} \gg 1$, the reliance of the signal on B_0 allows these DCs to be directly measured by removing the magnetic field, thereby suppressing systematic uncertainties, $\delta \ll 1$. In the statistically limited regime $\delta \ll 1/\sqrt{N_{\text{DC}}}$, an observable signal only needs to overcome Poisson fluctuations in noise, such that $g_{a\gamma} \propto (R_{\text{DC}}/M_{\text{T}}t)^{1/4}B_0^{-1}$. Below, we begin by discussing the sensitivity of various targets assuming negligible backgrounds and then proceed to examine the impact of currently measured noise sources.

For $m_a \gtrsim \text{eV}$, enough energy is deposited to excite an electron across the ~ 1 eV band gap in standard semiconductors, such as Si and Ge, which is then read out by drifting the charge to a sensing output. This is the operating principle of many ongoing experiments, such as CDEX [94], DAMIC [95–99], EDELWEISS [100–102], SENSEI [103–105], and SuperCDMS [106–108]. In our estimate of the signal rate in Eq. (2), we use the measured dielectric functions of Si and Ge from Ref. [128], and do not incorporate multiphonon responses at lower energies [80] since these are subdominant to the single-phonon responses of the polar materials discussed below. As shown in Fig. 1, background-free Ge targets have the potential to be the best laboratory-based search for the QCD axion for masses greater than that probed by the CAST helioscope [113,114] and smaller than that probed by astrophysical searches for $a \rightarrow 2\gamma$ decays [115–117].

While the energy of electronic excitations is limited to $\sim \text{eV}$ scales in standard semiconductors, novel targets have lower $\sim \text{meV}$ electronic excitations. For example, Dirac [61,63,65,69–72] and spin-orbit coupled materials [57,79] have small bulk band gaps. One such target that falls under both categories is ZrTe_5 ; while its Dirac character is somewhat debated [57], the presence of its small band gap has been firmly established [129]. However, since its dielectric response has not been accurately measured, we adopt the first-principles calculation performed in Ref. [57]. In addition to pure targets, doping is another method to create electronic states below the band gap.

Recently, Ref. [73] studied Si doped with phosphorus as a candidate target, using an analytic model for the dielectric response consistent with measurements [130,131]. In Fig. 1, we rescale their quoted dark photon sensitivity, using the mapping described above.

Phonon excitations [76,80,82–85,110] in the $\sim (1\text{--}100)$ meV energy range have also been studied as an avenue to detect axions [82,87]. The results shown in Fig. 1 are consistent with the first-principles calculation done in Ref. [82]. We have chosen to focus on GaAs, Al_2O_3 , and SiO_2 targets, as they are of active investigation in the sub-GeV DM community; the first two are currently planned for the TESSARACT experiment [111], and SiO_2 has also been identified as an optimal target for light DM scattering [76]. The measured dielectric data for these targets in the phonon energy regime is taken from Ref. [80].

Background.—The sensitivity of detectors focused on readout of single-electron excitations are currently limited by DCs [93]. The SENSEI experiment [104,132] utilizing a Si Skipper CCD detector, is the current state of the art for measuring charge from single-electron excitations. Recent measurements indicate a DC rate of $10^8/\text{kg yr}$ and $10^6/\text{kg yr}$ for energy ranges of $\lesssim 4.7$ eV and $\sim (4.7\text{--}8.3)$ eV, respectively, and rates consistent with zero for larger energies. Assuming that similar background levels in the two-electron bin can be achieved in a Ge-based detector, noise reduction by 3 orders of magnitude ($R_{\text{DC}} \sim 10^3/\text{kg yr}$) is necessary to attain sensitivity to the QCD axion at eV-scale masses. Similar noise levels, but at much lower energies, are also necessary for doped Si and ZrTe_5 targets to attain sensitivity to the QCD axion at ~ 100 meV masses.

Calorimetric detectors (e.g., SuperCDMS CPD [133], which measures phonons produced from single-electron excitations) have registered significantly higher noise levels $R_{\text{DC}} \sim 10^{10}/\text{kg yr}$. As an estimate of the backgrounds that will contaminate sensors based on detection of single-phonon excitations, we assume $R_{\text{DC}} = 10^{10}/\text{kg yr}$ and $\delta \lesssim 1/\sqrt{N_{\text{DC}}}$ for the dotted colored lines shown in Fig. 1. If the DCs are reduced to just $\sim 10^8/\text{kg yr}$ at ~ 100 meV energies, an Al_2O_3 or SiO_2 target can be sensitive to the QCD axion at couplings smaller than that bounded by considerations of stellar energy loss.

While their origin is unknown, noise levels are generally peaked toward smaller energies [134]. Recent work has focused on progressing the understanding of such backgrounds. For instance, it has been calculated that a subdominant fraction of DCs arises from secondary radiation generated by high-energy tracks [135] and photons [136] in low-threshold charge and phonon detectors, respectively. Additionally, a bulk of eV-scale phonon backgrounds in superconducting calorimetric detectors has recently been shown to emerge from cooling-induced microfractures in auxiliary detector components [137].

The setup investigated in our work differs from previously proposed applications of these targets in the use of a large external magnetic field, whose dominant effect will be disrupting detection technology based on superconducting devices (measurements of typical semiconducting sensors have found minor changes to their operation when exposed to ~ 1 T magnetic fields [138]). For example, transition edge sensors (TESs) (the main technology for reading out single-phonon excitations in the TESSARACT experiment) are not operative in $\gtrsim \mu\text{T}$ magnetic fields [139]. However, there is a strong dependence on the direction of the magnetic field relative to the face of the TES. Additionally, if the region of bulk target within the external magnetic field can be physically separated from the superconducting detector, these problems can be avoided. Other complications arising from, e.g., additional radioactive components or Lorentz-force-induced mechanical stress, may also be introduced. A detailed investigation of these effects is beyond the scope of this work, and these will also need to be confronted in other axion experiments operating in the meV–eV energy range [45,48]. However, we do not expect fundamental roadblocks in this approach since ~ 10 T magnetic fields only change electronic energies at the level of $\sim \text{meV}$, well below the energies investigated here.

Discussion.—The past decade has seen a meteoric rise in target proposals to hunt for sub-GeV DM. In an external magnetic field, these targets are also powerful probes of axions in a mass range that is notoriously difficult to explore, corresponding to $m_a \sim 10$ meV–10 eV. Searching for axions with these targets has the intrinsic advantage of directly utilizing all future experimental improvements in background reduction, an effort which has assiduously driven direct detection experiments to incredible precision in recent history. The axion absorption rate in a magnetized medium can be simply written in terms of the measurable dielectric function, encoding all in-medium responses. This synergizes with future developments toward optimizing the energy loss function of the material $\text{Im}(-1/\epsilon)$, as well as further study of other novel low-energy excitations, such as axion quasiparticles [140,141] or chiral phonons [142].

We would like to thank Aaron Chou, Juan Estrada, Roni Harnik, Yoni Kahn, Alex Millar, Tongyan Lin, Andrea Mitridate, Kris Pardo, and Kathryn Zurek for helpful conversations, and Ciaran O’Hare for the compilation of axion limits in Ref. [143]. This material is based upon work supported by the U.S. Department of Energy, Office of Science, National Quantum Information Science Research Centers, Superconducting Quantum Materials and Systems Center under Contract No. DE-AC02-07CH11359. Fermilab is operated by the Fermi Research Alliance, LLC under Contract No. DE-AC02-07CH11359 with the U.S. Department of Energy.

*aberlin@fnal.gov

†ttrickle@fnal.gov

- [1] P. A. Zyla *et al.* (Particle Data Group), Review of particle physics, *Prog. Theor. Exp. Phys.* **2020**, 083C01 (2020).
- [2] R. D. Peccei and H. R. Quinn, Constraints imposed by CP conservation in the presence of instantons, *Phys. Rev. D* **16**, 1791 (1977).
- [3] R. D. Peccei and H. R. Quinn, CP conservation in the presence of instantons, *Phys. Rev. Lett.* **38**, 1440 (1977).
- [4] F. Wilczek, Problem of strong P and T invariance in the presence of instantons, *Phys. Rev. Lett.* **40**, 279 (1978).
- [5] S. Weinberg, The $U(1)$ problem, *Phys. Rev. D* **11**, 3583 (1975).
- [6] P. Sikivie, Experimental tests of the invisible axion, *Phys. Rev. Lett.* **51**, 1415 (1983); **52**, 695(E) (1984).
- [7] C. B. Adams *et al.*, Axion dark matter, in *Proceedings of Snowmass 2021*, arXiv:2203.14923.
- [8] L. F. Abbott and P. Sikivie, A cosmological bound on the invisible axion, *Phys. Lett.* **120B**, 133 (1983).
- [9] M. S. Turner, Coherent scalar field oscillations in an expanding universe, *Phys. Rev. D* **28**, 1243 (1983).
- [10] M. S. Turner, Cosmic and local mass density of invisible axions, *Phys. Rev. D* **33**, 889 (1986).
- [11] J. Preskill, M. B. Wise, and F. Wilczek, Cosmology of the invisible axion, *Phys. Lett.* **120B**, 127 (1983).
- [12] M. Dine and W. Fischler, The not so harmless axion, *Phys. Lett.* **120B**, 137 (1983).
- [13] R. T. Co and K. Harigaya, Axionogenesis, *Phys. Rev. Lett.* **124**, 111602 (2020).
- [14] R. T. Co, L. J. Hall, K. Harigaya, K. A. Olive, and S. Verner, Axion kinetic misalignment and parametric resonance from inflation, *J. Cosmol. Astropart. Phys.* **08** (2020) 036.
- [15] R. T. Co, L. J. Hall, and K. Harigaya, Axion kinetic misalignment mechanism, *Phys. Rev. Lett.* **124**, 251802 (2020).
- [16] C. Hagmann, S. Chang, and P. Sikivie, Axions from string decay, *Nucl. Phys. B, Proc. Suppl.* **72**, 81 (1999).
- [17] M. Gorghetto, E. Hardy, and G. Villadoro, Axions from strings: The attractive solution, *J. High Energy Phys.* **07** (2018) 151.
- [18] R. A. Battye and E. P. S. Shellard, Axion string constraints, *Phys. Rev. Lett.* **73**, 2954 (1994); **76**, 2203(E) (1996).
- [19] M. Hindmarsh, J. Lizarraga, A. Lopez-Eiguren, and J. Urrestilla, Comment on “More axions from strings,” arXiv:2109.09679.
- [20] M. Dine, N. Fernandez, A. Ghalsasi, and H. H. Patel, Comments on “Axions, domain walls, and cosmic strings,” *J. Cosmol. Astropart. Phys.* **11** (2021) 041.
- [21] M. Buschmann, J. W. Foster, A. Hook, A. Peterson, D. E. Willcox, W. Zhang, and B. R. Safdi, Dark matter from axion strings with adaptive mesh refinement, *Nat. Commun.* **13**, 1049 (2022).
- [22] A. Vaquero, J. Redondo, and J. Stadler, Early seeds of axion miniclusters, *J. Cosmol. Astropart. Phys.* **04** (2019) 012.
- [23] M. Buschmann, J. W. Foster, and B. R. Safdi, Early-universe simulations of the cosmological axion, *Phys. Rev. Lett.* **124**, 161103 (2020).

- [24] V. B. Klaer and G. D. Moore, How to simulate global cosmic strings with large string tension, *J. Cosmol. Astropart. Phys.* **10** (2017) 043.
- [25] T. Hiramatsu, M. Kawasaki, T. Sekiguchi, M. Yamaguchi, and J. Yokoyama, Improved estimation of radiated axions from cosmological axionic strings, *Phys. Rev. D* **83**, 123531 (2011).
- [26] M. Gorghetto, E. Hardy, and G. Villadoro, More axions from strings, *SciPost Phys.* **10**, 050 (2021).
- [27] C.-F. Chang and Y. Cui, New perspectives on axion misalignment mechanism, *Phys. Rev. D* **102**, 015003 (2020).
- [28] K. Harigaya and J. M. Leedom, QCD axion dark matter from a late time phase transition, *J. High Energy Phys.* **06** (2020) 034.
- [29] R. T. Co, L. J. Hall, and K. Harigaya, QCD axion dark matter with a small decay constant, *Phys. Rev. Lett.* **120**, 211602 (2018).
- [30] M. Hindmarsh, J. Lizarraga, A. Lopez-Eiguren, and J. Urrestilla, Scaling density of axion strings, *Phys. Rev. Lett.* **124**, 021301 (2020).
- [31] R. Daido, F. Takahashi, and W. Yin, The ALP miracle: Unified inflaton and dark matter, *J. Cosmol. Astropart. Phys.* **05** (2017) 044.
- [32] R. Daido, F. Takahashi, and W. Yin, The ALP miracle revisited, *J. High Energy Phys.* **02** (2018) 104.
- [33] V. B. Klaer and G. D. Moore, The dark-matter axion mass, *J. Cosmol. Astropart. Phys.* **11** (2017) 049.
- [34] K.-S. Choi, H. P. Nilles, S. Ramos-Sanchez, and P. K. S. Vaudrevange, Accions, *Phys. Lett. B* **675**, 381 (2009).
- [35] B. S. Acharya, K. Bobkov, and P. Kumar, An M theory solution to the strong CP problem and constraints on the axiverse, *J. High Energy Phys.* **11** (2010) 105.
- [36] Y. Chikashige, R. N. Mohapatra, and R. D. Peccei, Are there real Goldstone bosons associated with broken lepton number?, *Phys. Lett.* **98B**, 265 (1981).
- [37] P. Svrcek and E. Witten, Axions in string theory, *J. High Energy Phys.* **06** (2006) 051.
- [38] C. D. Froggatt and H. B. Nielsen, Hierarchy of quark masses, Cabibbo angles and CP violation, *Nucl. Phys.* **B147**, 277 (1979).
- [39] R. T. Co, L. J. Hall, and K. Harigaya, Predictions for axion couplings from ALPogenesis, *J. High Energy Phys.* **01** (2021) 172.
- [40] E. Witten, Some properties of $O(32)$ superstrings, *Phys. Lett.* **149B**, 351 (1984).
- [41] A. Arvanitaki, S. Dimopoulos, S. Dubovsky, N. Kaloper, and J. March-Russell, String axiverse, *Phys. Rev. D* **81**, 123530 (2010).
- [42] J. P. Conlon, The QCD axion and moduli stabilisation, *J. High Energy Phys.* **05** (2006) 078.
- [43] M. Cicoli, M. Goodsell, and A. Ringwald, The type IIB string axiverse and its low-energy phenomenology, *J. High Energy Phys.* **10** (2012) 146.
- [44] J. Halverson, C. Long, and P. Nath, Ultralight axion in supersymmetry and strings and cosmology at small scales, *Phys. Rev. D* **96**, 056025 (2017).
- [45] J. Liu, K. Dona, G. Hoshino, S. Knirck, N. Kurinsky *et al.* (BREAD Collaboration), Broadband solenoidal haloscope for terahertz axion detection, *Phys. Rev. Lett.* **128**, 131801 (2022).
- [46] A. Caldwell, G. Dvali, B. Majorovits, A. Millar, G. Raffelt, J. Redondo, O. Reimann, F. Simon, and F. Steffen (MADMAX Working Group), Dielectric haloscopes: A new way to detect axion dark matter, *Phys. Rev. Lett.* **118**, 091801 (2017).
- [47] A. J. Millar, G. G. Raffelt, J. Redondo, and F. D. Steffen, Dielectric haloscopes to search for axion dark matter: Theoretical foundations, *J. Cosmol. Astropart. Phys.* **01** (2017) 061.
- [48] M. Baryakhtar, J. Huang, and R. Lasenby, Axion and hidden photon dark matter detection with multilayer optical haloscopes, *Phys. Rev. D* **98**, 035006 (2018).
- [49] M. Lawson, A. J. Millar, M. Pancaldi, E. Vitagliano, and F. Wilczek, Tunable axion plasma haloscopes, *Phys. Rev. Lett.* **123**, 141802 (2019).
- [50] A. Caputo, A. J. Millar, and E. Vitagliano, Revisiting longitudinal plasmon-axion conversion in external magnetic fields, *Phys. Rev. D* **101**, 123004 (2020).
- [51] A. J. Millar, S. M. Anlage, R. Balafendiev, P. Belov, K. van Bibber *et al.* (ALPHA Collaboration), Searching for dark matter with plasma haloscopes, *Phys. Rev. D* **107**, 055013 (2023).
- [52] Y. Hochberg, T. Lin, and K. M. Zurek, Absorption of light dark matter in semiconductors, *Phys. Rev. D* **95**, 023013 (2017).
- [53] G. Krnjaic and T. Trickle, Absorption of vector dark matter beyond kinetic mixing, *Phys. Rev. D* **108**, 015024 (2023).
- [54] A. Derevianko, V. A. Dzuba, V. V. Flambaum, and M. Pospelov, Axio-electric effect, *Phys. Rev. D* **82**, 065006 (2010).
- [55] R. Catena, T. Emken, M. Matas, N. A. Spaldin, and E. Urdshals, Crystal responses to general dark matter-electron interactions, *Phys. Rev. Res.* **3**, 033149 (2021).
- [56] A. Mitridate, T. Trickle, Z. Zhang, and K. M. Zurek, Dark matter absorption via electronic excitations, *J. High Energy Phys.* **09** (2021) 123.
- [57] H.-Y. Chen, A. Mitridate, T. Trickle, Z. Zhang, M. Bernardi, and K. M. Zurek, Dark matter direct detection in materials with spin-orbit coupling, *Phys. Rev. D* **106**, 015024 (2022).
- [58] R. Catena, D. Cole, T. Emken, M. Matas, N. Spaldin, W. Tarantino, and E. Urdshals, Dark matter-electron interactions in materials beyond the dark photon model, *J. Cosmol. Astropart. Phys.* **03** (2023) 052.
- [59] C. Blanco, J. I. Collar, Y. Kahn, and B. Lillard, Dark matter-electron scattering from aromatic organic targets, *Phys. Rev. D* **101**, 056001 (2020).
- [60] S. Knapen, J. Kozaczuk, and T. Lin, Dark matter-electron scattering in dielectrics, *Phys. Rev. D* **104**, 015031 (2021).
- [61] Y. Hochberg, M. Pyle, Y. Zhao, and K. M. Zurek, Detecting superlight dark matter with Fermi-degenerate materials, *J. High Energy Phys.* **08** (2016) 057.
- [62] Y. Hochberg, T. Lin, and K. M. Zurek, Detecting ultralight bosonic dark matter via absorption in superconductors, *Phys. Rev. D* **94**, 015019 (2016).
- [63] Y. Hochberg, Y. Kahn, M. Lisanti, K. M. Zurek, A. G. Grushin, R. Ilan, S. M. Griffin, Z.-F. Liu, S. F. Weber, and

- J. B. Neaton, Detection of sub-MeV dark matter with three-dimensional Dirac materials, *Phys. Rev. D* **97**, 015004 (2018).
- [64] Y. Hochberg, Y. Kahn, N. Kurinsky, B. V. Lehmann, T. C. Yu, and K. K. Berggren, Determining dark-matter–electron scattering rates from the dielectric function, *Phys. Rev. Lett.* **127**, 151802 (2021).
- [65] R. M. Geilhufe, F. Kahlhoefer, and M. W. Winkler, Dirac materials for sub-MeV dark matter detection: New targets and improved formalism, *Phys. Rev. D* **101**, 055005 (2020).
- [66] R. Essig, J. Mardon, and T. Volansky, Direct detection of sub-GeV dark matter, *Phys. Rev. D* **85**, 076007 (2012).
- [67] S. Derenzo, R. Essig, A. Massari, A. Soto, and T.-T. Yu, Direct detection of sub-GeV dark matter with scintillating targets, *Phys. Rev. D* **96**, 016026 (2017).
- [68] R. Essig, M. Fernandez-Serra, J. Mardon, A. Soto, T. Volansky, and T.-T. Yu, Direct detection of sub-GeV dark matter with semiconductor targets, *J. High Energy Phys.* **05** (2016) 046.
- [69] A. Coskuner, A. Mitridate, A. Olivares, and K. M. Zurek, Directional dark matter detection in anisotropic Dirac materials, *Phys. Rev. D* **103**, 016006 (2021).
- [70] Y. Hochberg, Y. Kahn, M. Lisanti, C. G. Tully, and K. M. Zurek, Directional detection of dark matter with two-dimensional targets, *Phys. Lett. B* **772**, 239 (2017).
- [71] R. Catena, T. Emken, M. Matas, N. A. Spaldin, and E. Urdshals, Direct searches for general dark matter–electron interactions with graphene detectors: Part I. Electronic structure calculations, *Phys. Rev. Res.* **5**, 043257 (2023).
- [72] R. Catena, T. Emken, M. Matas, N. A. Spaldin, and E. Urdshals, Direct searches for general dark matter–electron interactions with graphene detectors: Part II. Sensitivity studies, *Phys. Rev. Res.* **5**, 043258 (2023).
- [73] P. Du, D. Egaña Ugrinovic, R. Essig, and M. Sholapurkar, Doped semiconductor devices for sub-MeV dark matter detection, *Phys. Rev. D* **109**, 055009 (2024).
- [74] S. M. Griffin, K. Inzani, T. Trickle, Z. Zhang, and K. M. Zurek, Extended calculation of dark matter–electron scattering in crystal targets, *Phys. Rev. D* **104**, 095015 (2021).
- [75] T. Trickle, Extended calculation of electronic excitations for direct detection of dark matter, *Phys. Rev. D* **107**, 035035 (2023).
- [76] S. M. Griffin, K. Inzani, T. Trickle, Z. Zhang, and K. M. Zurek, Multichannel direct detection of light dark matter: Target comparison, *Phys. Rev. D* **101**, 055004 (2020).
- [77] T. Trickle, Z. Zhang, K. M. Zurek, K. Inzani, and S. M. Griffin, Multi-channel direct detection of light dark matter: Theoretical framework, *J. High Energy Phys.* **03** (2020) 036.
- [78] P. W. Graham, D. E. Kaplan, S. Rajendran, and M. T. Walters, Semiconductor probes of light dark matter, *Phys. Dark Universe* **1**, 32 (2012).
- [79] K. Inzani, A. Faghaninia, and S. M. Griffin, Prediction of tunable spin-orbit gapped materials for dark matter detection, *Phys. Rev. Res.* **3**, 013069 (2021).
- [80] S. Knapen, J. Kozaczuk, and T. Lin, PYTHON package for dark matter scattering in dielectric targets, *Phys. Rev. D* **105**, 015014 (2022).
- [81] P. Cox, T. Melia, and S. Rajendran, Dark matter phonon coupling, *Phys. Rev. D* **100**, 055011 (2019).
- [82] A. Mitridate, T. Trickle, Z. Zhang, and K. M. Zurek, Detectability of axion dark matter with phonon polaritons and magnons, *Phys. Rev. D* **102**, 095005 (2020).
- [83] S. Knapen, T. Lin, M. Pyle, and K. M. Zurek, Detection of light dark matter with optical phonons in polar materials, *Phys. Lett. B* **785**, 386 (2018).
- [84] A. Coskuner, T. Trickle, Z. Zhang, and K. M. Zurek, Directional detectability of dark matter with single phonon excitations: Target comparison, *Phys. Rev. D* **105**, 015010 (2022).
- [85] S. Griffin, S. Knapen, T. Lin, and K. M. Zurek, Directional detection of light dark matter with polar materials, *Phys. Rev. D* **98**, 115034 (2018).
- [86] T. Trickle, Z. Zhang, and K. M. Zurek, Effective field theory of dark matter direct detection with collective excitations, *Phys. Rev. D* **105**, 015001 (2022).
- [87] D. J. E. Marsh, J. I. McDonald, A. J. Millar, and J. Schütte-Engel, Axion detection with phonon-polaritons revisited, *Phys. Rev. D* **107**, 035036 (2023).
- [88] R. Barbieri, M. Cerdonio, G. Fiorentini, and S. Vitale, Axion to magnon conversion: A scheme for the detection of galactic axions, *Phys. Lett. B* **226**, 357 (1989).
- [89] G. Flower, J. Bourhill, M. Goryachev, and M. E. Tobar, Broadening frequency range of a ferromagnetic axion haloscope with strongly coupled cavity–magnon polaritons, *Phys. Dark Universe* **25**, 100306 (2019).
- [90] S. Chigusa, T. Moroi, and K. Nakayama, Detecting light boson dark matter through conversion into a magnon, *Phys. Rev. D* **101**, 096013 (2020).
- [91] T. Trickle, Z. Zhang, and K. M. Zurek, Detecting light dark matter with magnons, *Phys. Rev. Lett.* **124**, 201801 (2020).
- [92] A. Esposito and S. Pavaskar, Optimal anti-ferromagnets for light dark matter detection, *Phys. Rev. D* **108**, L011901 (2023).
- [93] R. Essig, G. K. Giovanetti, N. Kurinsky, D. McKinsey, K. Ramanathan, K. Stifter, and T.-T. Yu, Snowmass2021 Cosmic Frontier: The landscape of low-threshold dark matter direct detection in the next decade, in *Proceedings of Snowmass 2021* (Snowmass, 2021); arXiv:2203.08297.
- [94] Z. Y. Zhang *et al.* (CDEX Collaboration), Constraints on sub-GeV dark matter–electron scattering from the CDEX-10 experiment, *Phys. Rev. Lett.* **129**, 221301 (2022).
- [95] A. Aguilar-Arevalo, D. Amidei, D. Baxter, G. Canelo, B. A. Cervantes Vergara *et al.* (DAMIC Collaboration), Constraints on light dark matter particles interacting with electrons from DAMIC at SNOLAB, *Phys. Rev. Lett.* **123**, 181802 (2019).
- [96] I. Arnquist *et al.* (DAMIC-M Collaboration), First constraints from DAMIC-M on sub-GeV dark-matter particles interacting with electrons, *Phys. Rev. Lett.* **130**, 171003 (2023).
- [97] A. Aguilar-Arevalo, D. Amidei, X. Bertou, M. Butner, G. Canelo *et al.* (DAMIC Collaboration), First direct-detection constraints on eV-scale hidden-photon dark matter with DAMIC at SNOLAB, *Phys. Rev. Lett.* **118**, 141803 (2017).
- [98] A. Aguilar-Arevalo, D. Amidei, D. Baxter, G. Canelo, B. A. Cervantes Vergara *et al.* (DAMIC Collaboration), Results on low-mass weakly interacting massive particles

- from a 11 kg-day target exposure of DAMIC at SNOLAB, *Phys. Rev. Lett.* **125**, 241803 (2020).
- [99] J. R. T. de Mello Neto *et al.* (DAMIC Collaboration), The DAMIC dark matter experiment, *Proc. Sci.*, ICRC2015 (2016) 1221 [arXiv:1510.02126].
- [100] Q. Arnaud, E. Armengaud, C. Augier, A. Benoît, L. Bergé *et al.* (EDELWEISS Collaboration), First germanium-based constraints on sub-MeV dark matter with the EDELWEISS experiment, *Phys. Rev. Lett.* **125**, 141301 (2020).
- [101] E. Armengaud, C. Augier, A. Benoît, L. Bergé, J. Billard *et al.* (EDELWEISS Collaboration), Searches for electron interactions induced by new physics in the EDELWEISS-III germanium bolometers, *Phys. Rev. D* **98**, 082004 (2018).
- [102] E. Armengaud, C. Augier, A. Benoît, A. Benoit, L. Bergé *et al.* (EDELWEISS Collaboration), Searching for low-mass dark matter particles with a massive Ge bolometer operated above-ground, *Phys. Rev. D* **99**, 082003 (2019).
- [103] O. Abramoff, L. Barak, I. M. Bloch, L. Chaplinsky, M. Crisler *et al.* (SENSEI Collaboration), SENSEI: Direct-detection constraints on sub-GeV dark matter from a shallow underground run using a prototype skipper-CCD, *Phys. Rev. Lett.* **122**, 161801 (2019).
- [104] L. Barak, I. M. Bloch, M. Cababie, G. Canelo, L. Chaplinsky *et al.* (SENSEI Collaboration), SENSEI: Direct-detection results on sub-GeV dark matter from a new skipper-CCD, *Phys. Rev. Lett.* **125**, 171802 (2020).
- [105] M. Crisler, R. Essig, J. Estrada, G. Fernandez, J. Tiffenberg, M. S. Haro, T. Volansky, and T.-T. Yu (SENSEI Collaboration), SENSEI: First direct-detection constraints on sub-GeV dark matter from a surface run, *Phys. Rev. Lett.* **121**, 061803 (2018).
- [106] D. W. Amaral *et al.* (SuperCDMS Collaboration), Constraints on low-mass, relic dark matter candidates from a surface-operated SuperCDMS single-charge sensitive detector, *Phys. Rev. D* **102**, 091101 (2020).
- [107] R. Agnese *et al.* (SuperCDMS Collaboration), First dark matter constraints from a SuperCDMS single-charge sensitive detector, *Phys. Rev. Lett.* **121**, 051301 (2018); **122**, 069901(E) (2019).
- [108] Z. Ahmed *et al.* (CDMS Collaboration), Search for axions with the CDMS experiment, *Phys. Rev. Lett.* **103**, 141802 (2009).
- [109] M. F. Albakry *et al.* (SuperCDMS Collaboration), A strategy for low-mass dark matter searches with cryogenic detectors in the SuperCDMS SNOLAB facility, in *Proceedings of Snowmass 2021*; arXiv:2203.08463.
- [110] S. M. Griffin, Y. Hochberg, K. Inzani, N. Kurinsky, T. Lin, and T. C. Yu, Silicon carbide detectors for sub-GeV dark matter, *Phys. Rev. D* **103**, 075002 (2021).
- [111] C. Chang *et al.*, Snowmass 2021 letter of interest: The tessaract dark matter project, 2020.
- [112] M. J. Dolan, F. J. Hiskens, and R. R. Volkas, Advancing globular cluster constraints on the axion-photon coupling, *J. Cosmol. Astropart. Phys.* **10** (2022) 096.
- [113] S. Andriamonje *et al.* (CAST Collaboration), An improved limit on the axion-photon coupling from the cast experiment, *J. Cosmol. Astropart. Phys.* **04** (2007) 010.
- [114] V. Anastassopoulos *et al.* (CAST Collaboration), New cast limit on the axion-photon interaction, *Nat. Phys.* **13**, 584 (2017).
- [115] M. Regis, M. Taoso, D. Vaz, J. Brinchmann, S. L. Zoutendijk, N. F. Bouché, and M. Steinmetz, Searching for light in the darkness: Bounds on ALP dark matter with the optical MUSE-faint survey, *Phys. Lett. B* **814**, 136075 (2021).
- [116] P. Carena, G. Lucente, and E. Vitagliano, Probing the blue axion with cosmic optical background anisotropies, *Phys. Rev. D* **107**, 083032 (2023).
- [117] D. Grin, G. Covone, J.-P. Kneib, M. Kamionkowski, A. Blain, and E. Jullo, A telescope search for decaying relic axions, *Phys. Rev. D* **75**, 105018 (2007).
- [118] I. Shilon, A. Dudarev, H. Silva, and H. H. J. ten Kate, Conceptual design of a new large superconducting toroid for IAXO, the New International Axion Observatory, *IEEE Trans. Appl. Supercond.* **23**, 4500604 (2013).
- [119] The simplicity of this expression derives from the separability of the axion absorption process as $a + B_0 \rightarrow E$ followed by absorption of the corresponding electric field. This description is appropriate for the axion masses of interest here, such that the target size is much larger than the skin depth $\sim (m_a \text{Im}[\sqrt{\epsilon}])^{-1}$. In this case, the effects of boundary conditions (arising from, e.g., the finite size of the target or external electromagnetic shielding) can be ignored [51,120,121].
- [120] S. Chaudhuri, P. W. Graham, K. Irwin, J. Mardon, S. Rajendran, and Y. Zhao, Radio for hidden-photon dark matter detection, *Phys. Rev. D* **92**, 075012 (2015).
- [121] R. Balafendiev, C. Simovski, A. J. Millar, and P. Belov, Wire metamaterial filled metallic resonators, *Phys. Rev. B* **106**, 075106 (2022).
- [122] G. B. Gelmini, A. J. Millar, V. Takhistov, and E. Vitagliano, Probing dark photons with plasma haloscopes, *Phys. Rev. D* **102**, 043003 (2020).
- [123] E. Hardy and R. Lasenby, Stellar cooling bounds on new light particles: Plasma mixing effects, *J. High Energy Phys.* **02** (2017) 033.
- [124] S. Dubovsky and G. Hernández-Chifflet, Heating up the Galaxy with hidden photons, *J. Cosmol. Astropart. Phys.* **12** (2015) 054.
- [125] M. Pospelov, A. Ritz, and M. B. Voloshin, Bosonic super-WIMPs as keV-scale dark matter, *Phys. Rev. D* **78**, 115012 (2008).
- [126] A. Berlin, A. J. Millar, T. Trickle, and K. Zhou, Physical signatures of fermion-coupled axion dark matter, arXiv:2312.11601.
- [127] I. G. Irastorza and J. Redondo, New experimental approaches in the search for axion-like particles, *Prog. Part. Nucl. Phys.* **102**, 89 (2018).
- [128] D. W. Lynch and W. R. Hunter, *Handbook of Optical Constants of Solids* (Acad. Press, Boston, 1985).
- [129] L. Moreschini, J. C. Johannsen, H. Berger, J. Denlinger, C. Jozwiak, E. Rotenberg, K. S. Kim, A. Bostwick, and M. Grioni, Nature and topology of the low-energy states in ZrTe₅, *Phys. Rev. B* **94**, 081101(R) (2016).
- [130] A. Gaymann, H. P. Geserich, and H. v. Löhneysen, Temperature dependence of the far-infrared reflectance spectra

- of Si:P near the metal-insulator transition, *Phys. Rev. B* **52**, 16486 (1995).
- [131] A. Gaymann, H. P. Geserich, and H. v. Löhneysen, Far-infrared reflectance spectra of Si:P near the metal-insulator transition, *Phys. Rev. Lett.* **71**, 3681 (1993).
- [132] L. Barak, I. M. Bloch, A. Botti, M. Cababie, G. Cancelo *et al.* (SENSEI Collaboration), SENSEI: Characterization of single-electron events using a skipper charge-coupled device, *Phys. Rev. Appl.* **17**, 014022 (2022).
- [133] I. Alkhatib *et al.* (SuperCDMS Collaboration), Light dark matter search with a high-resolution athermal phonon detector operated above ground, *Phys. Rev. Lett.* **127**, 061801 (2021).
- [134] P. Adari *et al.*, EXCESS workshop: Descriptions of rising low-energy spectra, *SciPost Phys. Proc.* **9**, 001 (2022).
- [135] P. Du, D. Egana-Ugrinovic, R. Essig, and M. Sholapurkar, Sources of low-energy events in low-threshold dark-matter and neutrino detectors, *Phys. Rev. X* **12**, 011009 (2022).
- [136] K. V. Berghaus, R. Essig, Y. Hochberg, Y. Shoji, and M. Sholapurkar, Phonon background from gamma rays in sub-GeV dark matter detectors, *Phys. Rev. D* **106**, 023026 (2022).
- [137] R. Anthony-Petersen *et al.*, A stress induced source of phonon bursts and quasiparticle poisoning, [arXiv:2208.02790](https://arxiv.org/abs/2208.02790).
- [138] K. Kondo, T. Dotani, M. Ozaki, and M. Iwai, Performance improvement of x-ray ccds by applying a magnetic field, *Proc. SPIE Int. Soc. Opt. Eng.* **9144**, 91443W (2014).
- [139] M. de Wit, L. Gottardi, M. L. Ridder, K. Nagayoshi, E. Taralli, H. Akamatsu, D. Vaccaro, J.-W. A. den Herder, M. P. Bruijn, and J.-R. Gao, Mitigation of the magnetic field susceptibility of transition-edge sensors using a superconducting groundplane, *Phys. Rev. Appl.* **18**, 024066 (2022).
- [140] D. J. E. Marsh, K.-C. Fong, E. W. Lentz, L. Smejkal, and M. N. Ali, Proposal to detect dark matter using axionic topological antiferromagnets, *Phys. Rev. Lett.* **123**, 121601 (2019).
- [141] J. Schütte-Engel, D. J. E. Marsh, A. J. Millar, A. Sekine, F. Chadha-Day, S. Hoof, M. N. Ali, K.-C. Fong, E. Hardy, and L. Šmejkal, Axion quasiparticles for axion dark matter detection, *J. Cosmol. Astropart. Phys.* **08** (2021) 066.
- [142] C. P. Romao, R. Catena, N. A. Spaldin, and M. Matas, Chiral phonons as dark matter detectors, *Phys. Rev. Res.* **5**, 043262 (2023).
- [143] C. O'Hare, AxionLimits, <https://cajohare.github.io/AxionLimits/> (July 2020).